

Supporting Information for

Aligned N-doped Carbon Nanotube Bundles with Interconnected Hierarchical Structure as an Efficient Bi-functional Oxygen Electrocatalyst

Weiliang Tian^{1,3}, Cheng Wang⁵, Ruida Chen^{1,2}, Zhao Cai¹, Daojin Zhou^{1,2}, Yongchao Hao¹, Yingna Chang^{1,2}, Nana Han², Yaping Li¹, Junfeng Liu¹, Feng Wang^{1,*}, Wen Liu^{1,*}, Haohong Duan^{4,*} and XiaomingSun^{1,2}

¹ State Key Laboratory of Chemical Resource Engineering, Beijing University of Chemical Technology, Beijing100029, China.

² School of Energy, Beijing Advanced Innovation Center for Soft Matter Science, Beijing University of Chemical Technology, Beijing100029, China.

³ Key Laboratory of Chemical Resource Engineering in South Xinjiang, College of Life Science, Tarim University, Alar 843300, China.

⁴ Chemistry Research Laboratory, Department of Chemistry, University of Oxford, Oxford, OX1 3TA, United Kingdom.

⁵ Chinese Research Academy of Environmental Sciences, Beijing 100012, China.

*Corresponding author (email: wangf@mail.buct.edu.cn (Feng W); haohong.duan@chem.ox.ac.uk (Haohong D); wenliu@mail.buct.edu.cn (Wen Liu))

Experimental section:

The calculation of electron-transfer numbers: The number of electrons involved in the ORR

can be calculated from the Koutecky-Levich (K-L) equation:

$$(1) J^{-1} = J_L^{-1} + J_K^{-1} = (B\omega^{1/2})^{-1} + J_K^{-1}$$

$$(2) B = 0.62nFC_0(D_0)^{2/3}\nu^{-1/6}$$

$$(3) B = nFkC_0$$

$$(4) J_K^{-1} = J^{-1} - (0.62nFC_0(D_0)^{2/3}\nu^{-1/6}\omega^{1/2})^{-1}.$$

Where J is the measured current density, J_K and J_L are the kinetic- and diffusion-limiting current densities, ω is the angular velocity of the disk ($\omega = 2\pi N$, N is the linear rotation speed), n is the overall number of electrons transferred in oxygen reduction, F is the Faraday constant ($F = 96485 \text{ C mol}^{-1}$), C_0 is the bulk concentration of O_2 , ($C_0 = 1.2 \times 10^{-6} \text{ mol cm}^{-3}$), ν is the kinematic viscosity of the electrolyte ($\nu = 0.01 \text{ cm}^2 \text{ s}^{-1}$), D_0 is the diffusion coefficient of O_2 in 0.1 mol L^{-1} KOH ($1.9 \times 10^{-5} \text{ cm}^2 \text{ s}^{-1}$). According to equations (1) and (2), the number of electrons transferred (n) can be calculated to be 4.0, which indicates that the H-NCNTs lead to a four-electron-transfer reaction to reduce directly oxygen into OH^- .

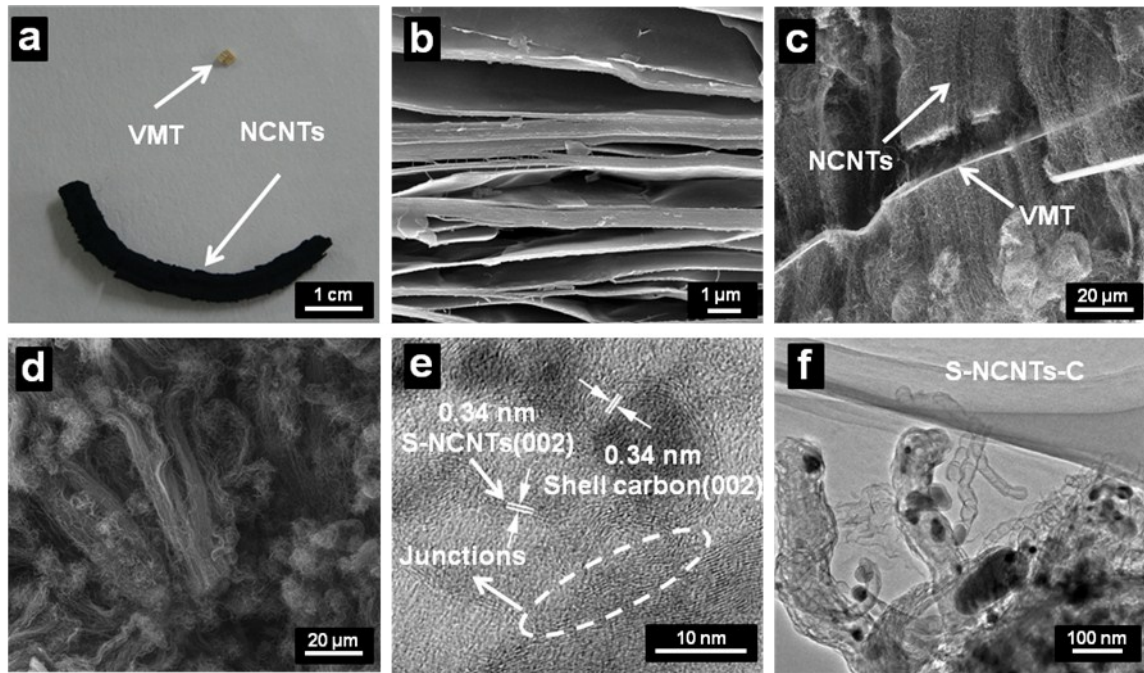


Figure S1. (a) Digital photograph of nature blocks of VMT and L-NCNTs/VMT. (b-d) Typical SEM images of VMT (b), L-NCNTs/VMT composites (c) and L-NCNTs after removal of VMT (d). (e, f) HRTEM images of h-NCNTs/Gr/TM (e) and S-NCNTs-C (f).

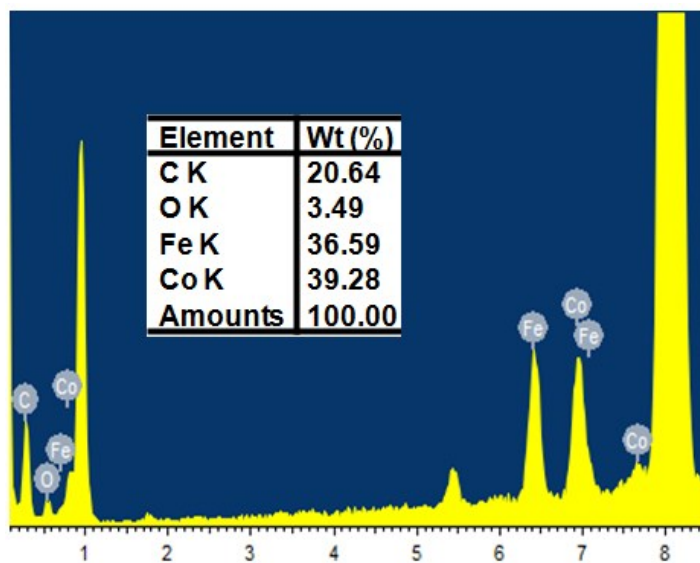


Figure S2. EDS spectrum for CoFe NPs in h-NCNTs/Gr/TM hybrid.

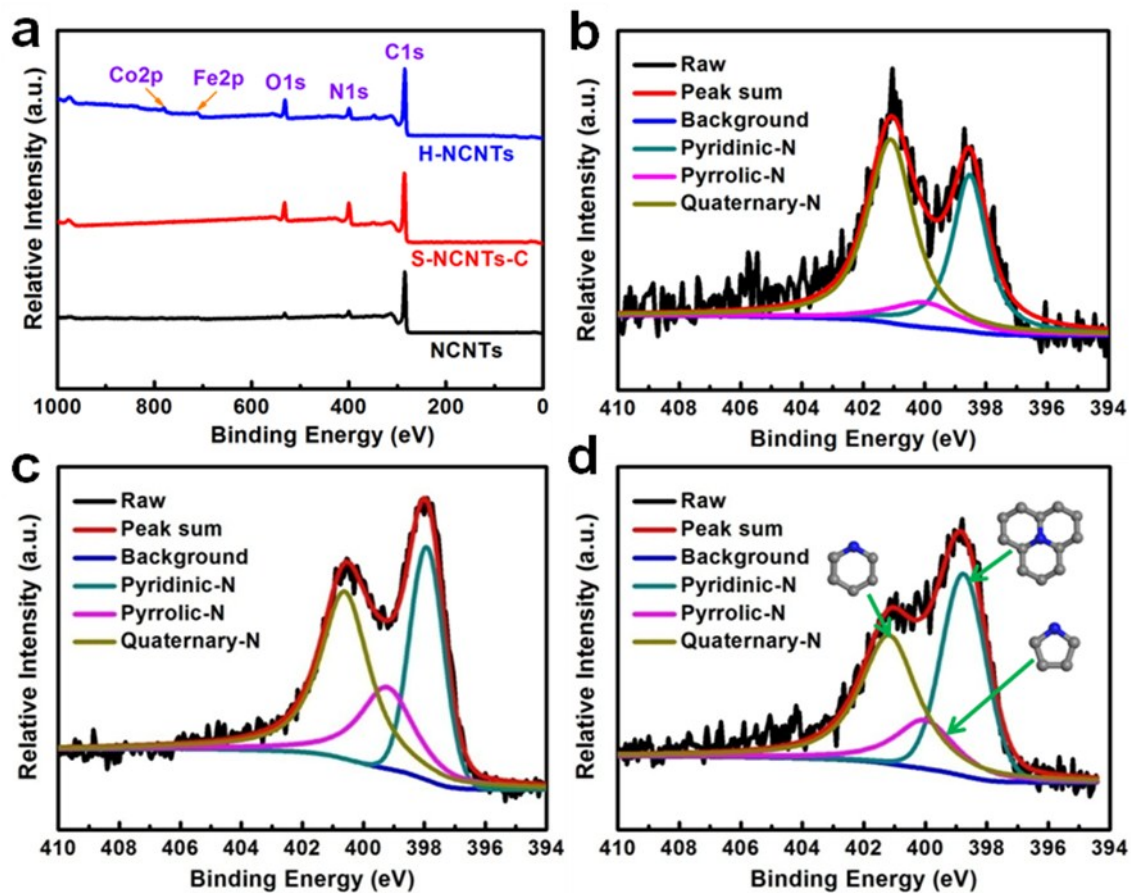


Figure S3. (a) XPS survey spectra of L-NCNTs, S-NCNTs-C, and h-NCNTs/Gr/TM; (b-d) N 1s binding energy region of L-NCNTs (b), S-NCNTs-C (c), and h-NCNTs/Gr/TM (d).

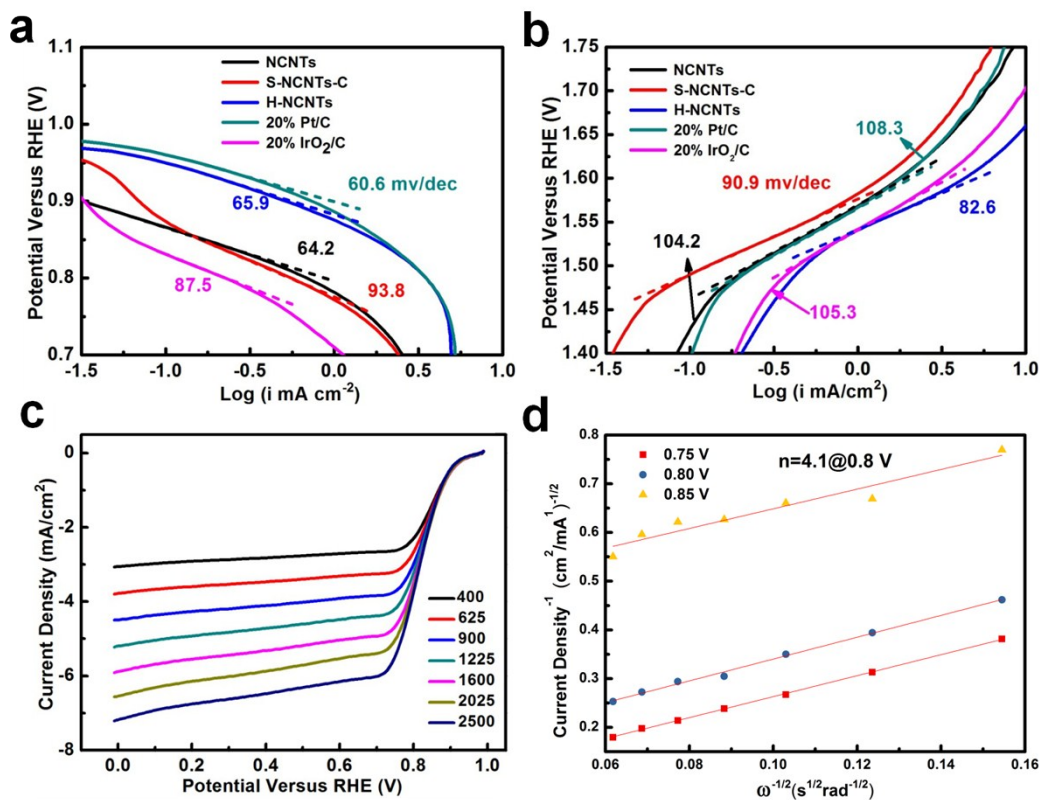


Figure S4. (a) ORR and (b) OER tafel plots of h-NCNTs/Gr/TM compared with L-NCNTs, S-NCNTs-C, Pt/C and IrO₂/C. Polarization curves (c) and K-L plots (d) of h-NCNTs/Gr/TM of ORR (Indicating the h-NCNTs/Gr/TM is four-electron-transfer reaction).

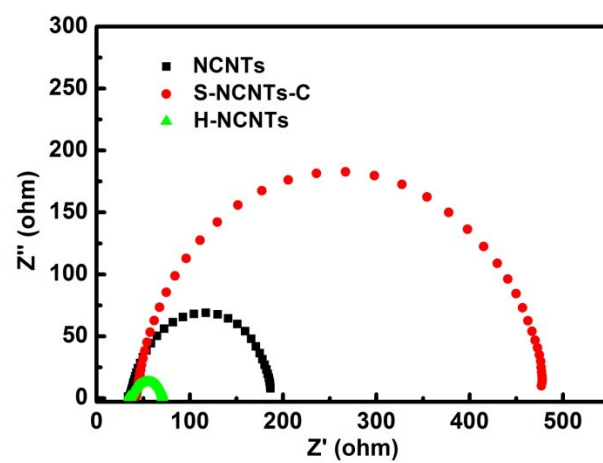


Figure S5. The electrochemical impedance spectra of h-NCNTs/Gr/TM, S-NCNTs-C and L-NCNTs.

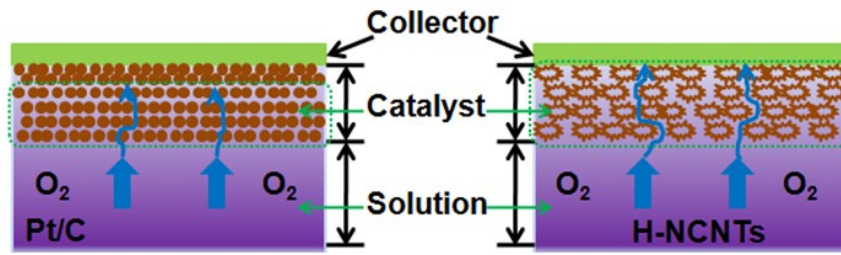


Figure S6. Graphical depiction of the transportation difference of solvated O₂ in catalyst layer of

Pt/C and h-NCNTs/Gr/TM occurring in ORR.

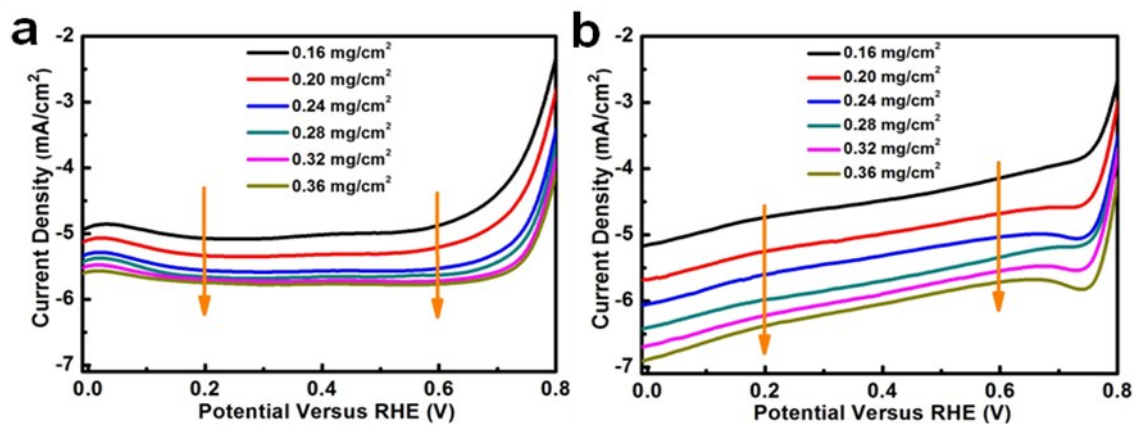


Figure S7. Investigations of the effect of catalyst's loading amount on ORR performance. (a) 20 wt% Pt/C and (b) h-NCNTs/Gr/TM.

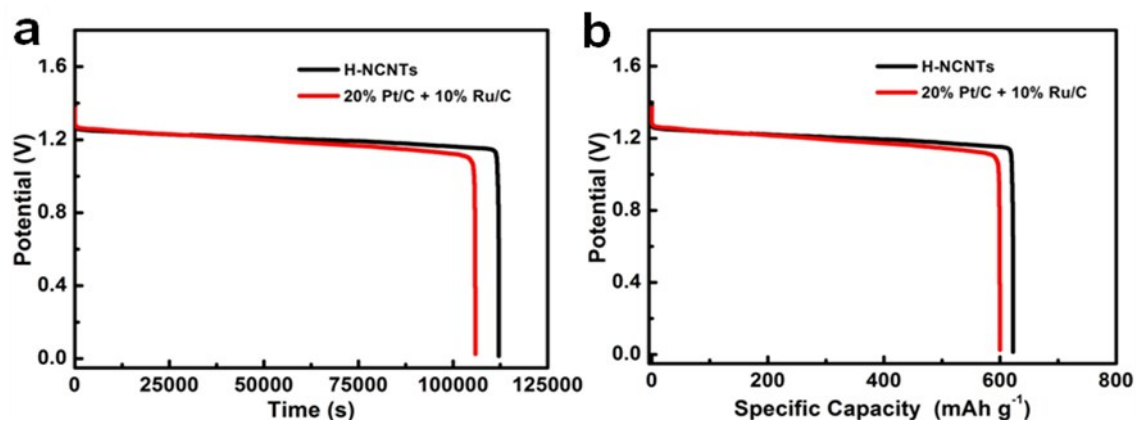


Figure S8. (a) The galvanostatic discharge curve of the primary zinc-air batteries at the current density of 7 mA cm⁻². (b) Specific capacities of the primary zinc-air batteries normalized to the mass of the consumed Zn at the current density of 7 mA cm⁻².

Table S1. The element content of L-NCNTs, S-NCNTs-C and h-NCNTs/Gr/TM obtained by XPS.

| L-NCNTs | Atomic (%) | S-NCNTs-C | Atomic (%) | h-NCNTs/Gr/TM | Atomic (%) |
|----------------|-------------------|------------------|-------------------|----------------------|-------------------|
| C1s | 93.99 | C1s | 81.68 | C1s | 88.18 |
| N1s | 6.01 | N1s | 16.91 | N1s | 9.73 |
| | | Fe2p3 | 1.68 | Co2p3 | 0.97 |
| | | | | Fe2p3 | 1.12 |

Table S2. Specific surface area and total pore volume of different samples.

| Sample | L-NCNTs | S-NCNTs-C | h-NCNTs/Gr/TM |
|---|----------------|------------------|----------------------|
| Specific surface area (m ² g ⁻¹) | 73.6 | 62.6 | 95.0 |
| Total pore volume (cm ³ g ⁻¹) | 0.23 | 0.15 | 0.25 |

Table S3. ORR and Zn-air battery performance of some carbon based system.

| Catalysts | Catalyst loading for ORR / Zn-air battery (mg cm ⁻²) ²⁾ | ORR Half-wave potential (V vs. RHE) | E _{gap} values (V@mA cm ⁻²) ²⁾ | Power density (mW cm ⁻²) | Reference |
|---|--|-------------------------------------|--|--------------------------------------|-----------|
| Co@N-CNT | 0.3728 / 2.5 | 0.805 | N/A | 244.0 | [1] |
| Co/N/O tri-doped graphene | 0.25 / 0.5 | 0.95 | 0.70@1 | 152 | [2] |
| Co-based metal hydroxysulfides | N/A | 0.721 | 1.12@5 | 113.1 | [3] |
| Cobalt-Based nanocomposites | 0.3 / 0.9 | 0.89 | 0.91@10 | 118.27 | [4] |
| FeCo-Nx -carbon nanosheets | N/A | 0.85 | 0.78@10 | 150 | [5] |
| Co, N-Codoped carbon nanoframes | 0.12 / N/A | 0.79 | 0.752@25 | N/A | [6] |
| Co-Nx-By-C carbon nanosheets | N/A / 0.5 | 0.83 | 0.83@10 | 100.4 | [7] |
| Strung Co ₄ N and Intertwined N-C Fibers | N/A | 0.8 | 0.84@10 | 174 | [8] |
| Nanoporous carbon Fiber Films | 0.1/0.1 | 0.8 | 0.73@10 | 185 | [9] |
| Transition metal and nitrogen co-doped carbon | 0.5 / 0.1 | 0.767 | 0.94@2 | N/A | [10] |
| This work | 0.5 / 2 | 0.81 | 0.6@5 | 81.76 | |

Reference:

1. H. Wu, X. Jiang, Y. Ye, C. Yan, S. Xie, S. Miao, G. Wang, X. Bao, *J. Energy Chem.* 2017, **26**, 1181.
2. C. Tang, B. Wang, H. Wang, Q. Zhang, *Adv. Mater.* 2017, **29**, 1703185.
3. H. Wang, C. Tang, B. Wang, B. Li, Q. Zhang, *Adv. Mater.* 2017, **29**, 1702327.
4. Y. Jiang, Y. Deng, J. Fu, D. U. Lee, R. Liang, Z. P. Cano, Y. Liu, Z. Bai, S. Hwang, L. Yang, D. Su, W. Chu, Z. Chen, *Adv. Energy Mater.* 2018, **8**, 1702900.
5. S. Li, C. Cheng, X. Zhao, J. Schmidt, A. Thomas, *Angew. Chem. Int. Ed.* 2018, **57**, 1856
6. Q. Wang, L. Shang, R. Shi, X. Zhang, Y. Zhao, G. I. N. Waterhouse, L. Wu, C. Tung, T. Zhang, *Adv. Energy Mater.* 2017, **7**, 1700467.
7. Y. Guo, P. Yuan, J. Zhang, Y. Hu, I. S. Amiinu, X. Wang, J. Zhou, H. Xia, Z. Song, Q. Xu, S. Mu, *ACS Nano.* 2018, **12**, 1894..
8. F. Meng, H. Zhong, D. Bao, J. Yan, X. Zhang, *J. Am. Chem. Soc.* 2016, **138**, 10226.

9. Q. Liu, Y. Wang, L. Dai, J. Yao, *Adv. Mater.* 2016, **28**, 3000.

10. B. Li, Y. Chen, X. Ge, J. Chai, X. Zhang, T. S. Andy Hor, G. Du, Z. Liu, H. Zhang, Y. Zong, *Nanoscale* 2016, **8**, 5067.